GROUND MOTION PREDICTION EQUATION FOR SPECTRUM INTENSITY BASED ON SPECTRAL ACCELERATION EQUATIONS

Brendon A Bradley*, Misko Cubrinovski, Gregory A MacRae, Rajesh P Dhakal.

Department of Civil Engineering, University of Canterbury, Private Bag 4800, Christchurch 8020, New Zealand

*Corresponding author: Ph +64-3-366 7001 ext 7673; Fax: +64-3-364 2758;

Email: bab54@student.canterbury.ac.nz

ABSTRACT

Spectrum intensity (*SI*) defined as the integral of the pseudo spectral velocity of a ground motion from 0.1 to 2.5 seconds, has recently been shown to be an intensity measure that efficiently predicts the seismic response of both liquefiable and non-liquefiable soil deposits, as well as the seismic demands on pile foundations embedded in such deposits. In order for such an intensity measure to be used in performance-based assessment and design, ground motion prediction relations are required to develop ground motion hazard curves in terms of *SI* for various sites. As such relationships developed specifically for *SI* are sparse, the authors propose the development of a relationship based on current ground motion prediction relations for spectral acceleration, which are available in most regions of seismic activity. Comparison with a direct prediction equation for *SI* provides a validation of the proposed approach. It is illustrated that *SI* is an intensity measure with a good predictability, thereby further promoting its attractiveness for use in reliability-based seismic response analysis.

KEYWORDS

Seismic response analysis; Spectrum intensity (*SI*); Spectral acceleration (*Sa*); Intensity measure (IM); Seismic hazard; Efficiency; Predictability.

INTRODUCTION

The seismic demand on structures due to ground motion excitation is highly uncertain due to the inherently random nature of the fault rupture process, seismic wave propagation and local site effects, as well as the variation in the seismic response of structures subjected to ground motion excitations of similar intensity. The latter indicates that in such seismic response analysis it is important to employ a ground motion intensity measure (IM) which is *efficient* (Shome and Cornell, 1999) in predicting these seismic demands. The former indicates however, that consideration should also be given to the *predictability* (Kramer and Mitchell, 2006) of the IM, which relates to the ability of the IM to be predicted from available ground motion prediction equations. Such a ground motion prediction equation is required to determine the ground motion hazard curve for a specific site, allowing determination of the temporal occurrence of the adopted ground motion IM. In addition to having a ground motion prediction equation for a specified IM, it is also desirable that the prediction equation has a high predictability (i.e. a relatively small variation in the ground motion intensity for a given earthquake scenario) which influences the ground motion hazard curve determined via probabilistic seismic hazard analysis (PSHA). Kramer and Mitchell (2006) illustrate how significant uncertainty in the ground motion prediction model of the IM causes an increase in the ground motion hazard and this in turn results in an increase in the demand hazard. In other words, if the *predictability* of an IM is poor, then the accuracy in predicting the seismic response (for a given earthquake scenario) will also be poor.

Recent research (Bradley *et al.*, 2008a, 2008b) has suggested that Spectrum Intensity (*SI*) is an *efficient* predictor of the seismic response of soil deposits, both for liquefiable and non-liquefiable soils, as well as the seismic demands of pile foundations embedded in such soil deposits. As mentioned above, however, in order for *SI* to be routinely used in performance-based assessment and design, ground motion prediction relations are required to

develop ground motion hazard curves in terms of *SI* at various sites of interest. Such relationships developed specifically for *SI* are sparse, thus limiting the potential application of *SI* in performance-based seismic assessments.

This paper introduces an indirect method for development of a ground motion prediction equation for *SI* based on ground motion prediction equations for spectral accelerations which are available in abundance. The formulation presented herein allows computation of *SI* based on any spectral acceleration (*Sa*) prediction equation as well as to incorporate specific features of individual *Sa* prediction models.

SPECTRUM INTENSITY PREDICTION EQUATION

Spectrum intensity, *SI*, originally proposed by Housner (1952; 1963) is defined as the integral of the pseudo-spectral velocity (*PSV*) over the period range of 0.1-2.5 seconds as given by Equation (1). In general, *SI*, is defined for any level of viscous damping, however commonly a value of 5% of the critical damping is selected, and will be adopted here.

$$SI = \int_{0.1}^{2.5} PSV(\mathrm{T},5\%)\mathrm{dT} \qquad 1)$$

The following section presents a method from which a ground motion prediction equation for *SI* can be determined from ground motion prediction equations for spectral acceleration, (*Sa*), which are readily available and well developed.

In general, ground motion prediction equations for spectral accelerations provide the median (50^{th} percentile) spectral acceleration and an associated lognormal standard deviation. The lognormal standard deviation is typically provided as it has been shown by various researchers that spectral accelerations are approximately lognormally distributed (Jayaram and Baker, 2008).

In order to compute the ground motion prediction equation for *SI* as proposed in this paper, it will be necessary to make use of the non-log form for the (statistical) moments of the

spectral acceleration ordinates. Thus, Equations (2) and (3), which are properties of the lognormal distribution, can be used to obtain the non-log moments of the spectral acceleration prediction equation:

$$\mu_{Sa} = Sa_{50} \exp\left(\frac{1}{2}\sigma^2_{\ln Sa}\right) \tag{2}$$

$$\sigma_{Sa} = \mu_{Sa}\sqrt{\exp\left(\sigma^2_{\ln Sa}\right)-1} \tag{3}$$

where Sa_{50} and $\sigma_{\ln Sa}$ are the median and lognormal standard deviation of the spectral acceleration, determined directly from *Sa* prediction equations; and μ_{Sa} and σ_{Sa} are the (non-log form) mean and standard deviation of the spectral acceleration, respectively.

Further noting that the pseudo-spectral velocity is related to the spectral acceleration by:

$$PSV(T_i) = \frac{Sa(T_i)}{\omega_i} = \frac{Sa(T_i).T_i}{2\pi} \tag{4}$$

then the mean and standard deviation of *PSV* for a given earthquake scenario (magnitude, distance, fault style and site conditions) and vibration period can be obtained from:

$$\mu_{PSV_i} = \mu_{Sa_i} / \omega_i \tag{5}$$

$$\sigma^2_{PSV_i} = \sigma^2_{Sa_i} / \omega_i^2 \tag{6}$$

Replacing the integral of Equation (1) with a discrete summation approximation gives:

$$SI = \Delta T \sum_{i=1}^{n} w_i PSV(\mathrm{T_i},5\%) \tag{7}$$

where n = the number of periods (from 0.1 to 2.5 seconds) that *PSV* is computed at; ΔT is the size of the vibration period discretization (the step-size used in the integration); and w_i are integration weights which depend on the integration scheme used. From Equation (7), the mean and variance of *SI* can then be computed from (Ang and Tang, 1975):

$$\mu_{SI} = \Delta T \sum_{i=1}^{n} w_i \mu_{PSV_i} \tag{8}$$

$$\sigma_{SI}^2 = (\Delta T)^2 \sum_{i=1}^{n} \sum_{j=1}^{n} \left(w_i w_j \rho_{PSV_i, PSV_j} \sigma_{PSV_i} \sigma_{PSV_j} \right) \quad (9)$$

where $PSV_i = PSV(T_i, 5\%)$; μ_{PSV_i} and $\sigma_{PSV_i}^2$ are the mean and variance, respectively, of the *PSV* ground motion prediction equation; and ρ_{PSV_i, PSV_j} is the correlation between PSV_i and PSV_j, i.e. the correlation between the *PSV* at two different vibration periods. Note that Equations (8) and (9) is exact, irrespective of the distribution of the spectral velocity terms. However, Equations (8) and (9) provide only the first two (statistical) moments of *SI* and no information on the resulting distribution of *SI*.

Again it is noted that as $PSV_i = Sa_i/\omega_i$, where ω is the circular natural frequency, then it can be shown that (see Appendix):

$$\rho_{PSV_i, PSV_j} = \rho_{Sa_i, Sa_j} = \frac{\exp\left(\rho_{\ln Sa_i, \ln Sa_j} \sigma_{\ln Sa_i} \sigma_{\ln Sa_j}\right) - 1}{\sqrt{\exp\left(\sigma_{\ln Sa_i}^2\right) - 1} \sqrt{\exp\left(\sigma_{\ln Sa_j}^2\right) - 1}} \approx \rho_{\ln Sa_i, \ln Sa_j} \quad (10)$$

where ρ_{Sa_i, Sa_j} is the correlation between spectral accelerations at vibration periods *i* and *j*; and $\rho_{\ln Sa_i, \ln Sa_j}$ is the correlation between the logarithm of spectral accelerations at vibration periods *i* and *j*. Equation (10) illustrates that the correlation between two different spectral velocities is equivalent to the correlation between two different spectral acceleration terms, and is a first order approximation to the correlation between the logarithm of two different spectral acceleration terms (although note that the exact expression for the relationship between log and non-log correlations is used herein unless otherwise stated).

Numerous spectral acceleration relationships can therefore be used to compute the mean and standard deviation of *Sa* (which can then be converted to *PSV*), while several models are available for $\rho_{\ln Sa_i, \ln Sa_j}$ (Baker and Cornell, 2006; Baker and Jayaram, 2008; Inoue and Cornell, 1990).

Equations (8) and (9) gives the two (non-log) moments for *SI* and if it is assumed that

the distribution of *SI* can be adequately represented by the lognormal distribution (which is shown to be the case later in this manuscript) then the median and lognormal standard deviation can be computed from re-arranged forms of Equations (2) and (3):

$$SI_{50} = \frac{\mu_{SI}^2}{\sqrt{\sigma_{SI}^2 + \mu_{SI}^2}} \tag{11}$$

$$\sigma_{\ln SI} = \sqrt{\ln\left(\left(\frac{\sigma_{SI}}{\mu_{SI}}\right)^2 + 1\right)} \tag{12}$$

where μ_{SI} and σ_{SI} are obtained from Equations (8) and (9), respectively, and SI_{50} and $\sigma_{\ln SI}$ are the median and lognormal standard deviation (dispersion) of the spectrum intensity of a ground motion produced for a given scenario. Equations (11) and (12) can be used directly in conventional *PSHA* computer programs. The principal benefit of computation of *SI* directly from spectral acceleration prediction equations comes from the significantly advanced state of *Sa* prediction equations in regard to quantification of faulting styles and site conditions, and large databases of empirical data used for their calibration (e.g. Abrahamson and Silva, 2008; Boore and Atkinson, 2008; Campbell and Bozorgnia, 2008).

DISTRIBUTION OF SI PREDICTION EQUATION

The previous section illustrated how the (non-log form) mean and standard deviation of the spectrum intensity can be determined from spectral acceleration prediction equations. However, it was also mentioned that while the mean and standard deviation are correct using Equations (8) and (9), respectively, no information is given regarding the distribution of *SI*. In what follows, the distribution of *SI* using the proposed approach presented in the previous section is investigated.

In order to determine the distribution shape of *SI*, a Monte-carlo scheme is used to: (i) randomly generate correlated logarithmic spectral acceleration amplitudes at various periods;

(ii) take the exponent of the logarithmic terms to obtain (non-log) *Sa* terms; (iii) convert to pseudo-spectral velocities using Equation (4); and (iv) compute the spectrum intensity, *SI*. These four steps are further elaborated below.

Step 1: Generate correlated logarithmic spectral acceleration terms

As spectral accelerations are known to be correlated at various periods, then random generation of vectors of spectral acceleration terms involves generating correlated random variables. It has already been mentioned that logarithmic spectral acceleration ordinates have been shown by various researchers to be normally distributed. In addition, Jayaram and Baker (2008) illustrate that logarithmic spectral acceleration terms are not only marginally, but also jointly normally distributed. Thus, it is possible to generate the logarithmic spectral acceleration terms using a multivariate normal distribution with correlation matrix as defined by an empirical equation for $\rho_{\ln Sa_i, \ln Sa_j}$. Herein, unless otherwise noted, the Boore and Atkinson (2008) NGA ground motion prediction equation for spectral acceleration, and the Jayaram and Baker (2008) correlation model are used, both of which were developed using the same ground motion database.

Step 2: Convert to non-log spectral acceleration

The correlated logarithmic spectral acceleration terms in the previous section can be simply converted to (non-log) spectral accelerations using:

$$Sa_i^k = \exp\left(\ln Sa_i^k\right) \quad (13)$$

where $\ln Sa_i^k = \ln Sa(T = T_i, 5\%)^k$ is the logarithmic spectral acceleration at vibration period T_i, generated during realisation k; and Sa_i^k is the non-log form of $\ln Sa(T = T_i, 5\%)^k$.

Steps 3&4: Convert to spectral velocity and compute SI_i

Once the vector of Sa_i^k terms have been obtained, Equation (4) can be used to obtain a vector of pseudo-spectral velocity terms. Equation (7) can then be used to compute the

spectrum intensity for realization *k*.

Resulting distribution

Figure 1 illustrates a comparison of the distribution of *SI* obtained using the simulation procedure described above with the lognormal and normal analytic distributions obtained based on the moments computed using Equations (8) and (9). The figure is based on a $M_w = 6.5$ strike-slip rupture at a distance of 30 km from a site with a 30m-weighted-average shear wave velocity of $V_{s(30)} = 300$ m/s. The simulation is based on 10000 realisations using the approach outlined in the previous section. In both the simulation and the analytic method (using Equations (8) and (9) for the normal distribution and Equations (11) and (12) for the lognormal distribution) a vibration period discretization of 0.1 seconds was adopted, (the vibration period discretization is discussed later in the manuscript). It can be seen that the lognormal distribution provides an excellent approximation to the results of the simulation while the normal distribution provides a poor fit. It is worth noting here that while the central limit theorem (Ang and Tang, 1975) may intuitively suggest that as the vibration period discretization becomes significantly small (i.e. the number of terms in the summation in Equations (8) and (9) become significantly large) then the resulting distribution for *SI* would approach the normal distribution (in the case of $\Delta T = 0.1$, there are 25 terms in the summation). However, as illustrated by the results of the simulation the central limit theorem does not apply here. This is primarily due to the high linear dependence (correlation) between the spectral acceleration terms at different vibration periods. Although not shown here, it was verified by the authors that reducing the vibration period discretization as low as $\Delta T = 0.01$, such that there are 250 spectral acceleration terms in Equation (7), did not affect the resulting distribution of *SI*.

As previously noted Equations (8) and (9) have been used to obtain the moments for *SI*, which have then been used to obtain the normal and lognormal distributions shown in Figure

1. Figure 2a illustrates the error in the prediction of the mean and standard deviation using Equations (8) and (9) relative to the results of the simulation. Because of the random nature of the simulations, multiple simulations (20 in this case) each with 10000 realizations were used to obtain cumulative distributions of the relative errors. It can be seen that the prediction of the mean *SI* from Equation (8) is accurate with the majority of the 20 different simulations giving an absolute relative error of less than 0.5%. The distribution of the relative error in the standard deviation is also centered around zero, but with a slightly larger scatter than that of the mean (if the first order approximation is made for the correlation (Equation (10)) there is a bias in the standard deviation of approximately 2.5%).

Figure 2b illustrates the variation in the Kolmogorov-Smirnov (KS) test statistic (Ang and Tang, 1975) over the 20 different simulations performed. The KS statistic gives the maximum difference between the empirical (from simulation) and analytical (lognormal) distributions over all the range of spectrum intensity values obtained. Thus Figure 2b indicates that over the entire range of *SI* values, the maximum difference between the empirical distribution and the lognormal distribution is typically about 0.011. The KS critical test statistic value for n = 10000 simulations is also shown for a confidence level of $\alpha = 5\%$. The fact that 80% of the simulations performed fall within the KS critical value indicates further that while the lognormal distribution is not exact, the assumption is relatively good.

Because the scale used in the KS test is arithmetic, it is unlikely that the value of the statistic is obtained near the tails of the distributions (Ang and Tang, 1975). Thus, separate attention should be devoted to the inspection of the tails of the empirical distribution. Figure 3a illustrates the comparison between the tails of the empirical and lognormal distributions for the same simulation as shown in Figure 1. It can be seen that the comparison between the empirical distribution from simulation and the lognormal distribution based on Equations (8) and (9) is good over the full tail of the *SI* distribution. The Anderson-Darling (AD) goodness-

of-fit test (Ang and Tang, 1975) is one such test for testing the tails of empirical distributions. In similar fashion to the KS statistic computed above, 20 different simulations using 10000 realisations were used to compute the empirical distribution for the AD test statistic shown in Figure 3b. Also for comparison the critical AD test statistic for a confidence level of 5% is shown. The fact that approximately 90% of the 20 simulations gave an AD test statistic less than the critical indicates the adequacy of the lognormal distribution in describing the tails of the *SI* distribution.

This section has investigated the assumption of lognormality for the distribution of *SI* obtained based on Equations (8) and (9). It has been illustrated that both the 'body' and 'tail' of the distribution conform to the lognormal distribution based on statistical tests. While there is some small error between the empirical and lognormal distributions, it should be realised that the assumption that spectral accelerations are lognormally distributed, although shown to be valid, is still an assumption. Also, the error induced in assuming that *SI* is lognormally distributed is likely to be negligible compared to the variation in ground motion due to epistemic uncertainties associated with earthquake rupture forecasts (ERFs) and the functional forms for spectral acceleration attenuation relationships themselves.

EFFECT OF VIBRATION PERIOD DISCRETIZATION

The discrete form for the computation of *SI*, as given by Equation (7) requires the size of the vibration period discretization, ΔT, to be selected in order to (discretely) obtain *SI* from the integral of the pseudo-velocity spectra. The selection of the discretization size will have an effect on both the median and dispersion (lognormal standard deviation) obtained using Equations (11) and (12) (as will the selection of the numerical integration method used, which affects the integration weights, w_i).

Since empirical ground motion prediction equations use regression to determine the

distribution of spectral acceleration at a discrete range of periods, then interpolation is required to determine the distribution of spectral ordinates at periods other than those for which empirical coefficients are determined for. The simplest and most common form of interpolation in such cases is linear interpolation, and is therefore adopted here. Because linear interpolation is used to determine the distribution of spectral accelerations at various periods, it seems appropiate that the Trapezoidal rule is used to evaluate Equation (1), which also makes use of linear interpolation between integration points. Thus, using the Trapezoidal rule in the form of Equation (7), the integration weights, w_i, will take the value of 0.5 for i=1 and n, and 1.0 otherwise.

Figure 4 illustrates the convergence of the median and dispersion for *SI* using the proposed approach. A range of discretization sizes from 1.2s (giving 3 *Sa* points), through to 0.01s (giving 250 *Sa* points), were considered. Figure 4 illustrates that, as expected, convergence is achieved as the discretization size is reduced, and that a step size below ΔT = 0.2s is appropriate for a wide range of magnitude and distance scenarios (two of which are shown here).

PROPERTIES OF *SI* PREDICTION EQUATION

Comparison with direct prediction of *SI*

It is of interest to compare the prediction of *SI* based on a prediction relationship for *SI*, with the prediction of *SI* obtained via prediction equations for *Sa*, which is the focus of this study. Danciu and Tselentis (2007) present ground motion prediction equations for various ground motion intensity measures for predominantly shallow earthquake ruptures in Greece of normal and thrust focal mechanisms. The ground motion intensity measures considered include both spectrum intensity, *SI*, and spectral acceleration, *Sa*. Danciu and Tselentis (2007) use a slightly modified version of *SI* than that presented here, their version having a

'normalising' factor of '1/2.4' at the front of the integral given in Equation (1). It is a trivial matter to multiply the results obtained from Danciu and Tselentis (2007) by 2.4 to obtain those results presented herein. In addition, the standard deviations given by Danciu and Tselentis (2007) are in terms of the base 10 logarithm ($\log_{10}$), and are converted to natural logarithms (ln) using a scaling factor of ln(10). Figure 5 illustrates the comparison between the median, 16th and 84th percentiles of the spectrum intensity distribution for a $M_w = 6.5$ normal fault rupture at various distances from a rock site. It is evident from the figure that the median spectrum intensities obtained using the two different approaches are practically identical, while there is a minor under-prediction of the magnitude of the dispersion.

Size of lognormal standard deviation of *SI*

As was mentioned in the introduction of this manuscript, it is desirable to have a ground motion intensity measure (IM) which is both *efficient* in predicting the response of a structure due to ground motion excitation, and *predictable* in the sense that a ground motion prediction equation exists which can estimate the IM with a low (relative to alternate IMs) uncertainty for a given earthquake scenario. Thus it is pertinent to investigate the predictability of *SI* in comparison to other common IMs such as peak ground velocity (*PGV*), and *Sa*. Figure 6 provides a comparison between the dispersions of the three aforementioned IMs using the Boore and Atkinson (2008) NGA prediction equation for computation of *Sa* and *PGV*, and the proposed approach for computing *SI* with the Boore and Atkinson prediction equation for *Sa*. As is generally observed in spectral acceleration prediction equations the dispersion increases as the period of vibration increases, while *PGV* and *SI* are obviously independent of vibration period. Both *PGV* and *SI* are observed to be more *predictable* than the *Sa* terms. For *SI* in particular, this is due to the fact that spectral acceleration terms are not perfectly correlated at various vibration periods, which reduces that standard deviation in *SI* compared to the case of perfectly correlated *Sa* terms (e.g. Equation (12)).

Variation in dispersion with magnitude and distance

In addition to the dispersion in the spectral acceleration ground motion prediction equations being a function of the vibration period, historically dispersion in ground motion prediction equations were also a function of earthquake rupture magnitude (e.g. Abrahamson and Silva, 1997; Campbell and Bozorgnia, 1994), with the dispersion reducing as the magnitude increased; but were generally assumed to be independent of source-to-site distance. However, in the recent release of the NGA ground motion equations (e.g. Abrahamson and Silva, 2008; Boore and Atkinson, 2008; Campbell and Bozorgnia, 2008), some prediction equation developers appear to have decided that in the revised models, the magnitude dependence is insignificant, and therefore have been determined independent of rupture magnitude.

Because the computation of *SI* proposed here does not enforce any dependence/independence of the dispersion on magnitude or distance, it is possible that the *SI* prediction is dependent on magnitude and distance, even if the *Sa* prediction is not. Figure 7 illustrates the variation in dispersion as a function of both magnitude and (Boore-Joyner) distance using the Boore and Atkinson (2008) NGA prediction equation. Figure 7a illustrates that the dispersion is observed to increase as the (moment) magnitude increases, the opposite trend in comparison to the magnitude-dependent dispersion for spectral acceleration terms. This increasing trend is however relatively insignificant, providing an increase from 0.55 for $M_w = 5$ to 0.60 for $M_w = 8$ (8.3% increase) in comparison to the variation in dispersion of 0.38-0.545 (30.3% increase) from $M_w = 5$ to 7.4 used in Campbell and Bozorgnia (1994). Figure 7b illustrates the dependence of the dispersion on source-to-site distance for the particular fault rupture scenario considered. In this case, there is evidently no dependence on the source-to-site distance with the dispersion ranging from approximately 0.58-0.587.

CONCLUSIONS

Seismic response analysis of structures requires the use of ground motion intensity measures which both *efficiently* predict the seismic response of structure due to ground motion excitation, and are *predictable* in the sense that a ground motion prediction equation exists which can estimate the IM with a relatively low uncertainty for a given earthquake rupture scenario. It this paper a ground motion prediction equation for spectrum intensity (*SI*), defined as the integral of the pseudo-velocity spectra over the 0.1-2.5s period range, has been proposed based on spectral acceleration (*Sa*) prediction equations, which are both extensively developed and abundant in research publications and earthquake engineering practice. The theoretical basis behind the development of the *SI* prediction equation based on *Sa* prediction equations was presented and various pertinent issues relating to its development were addressed. In particular, it was shown that the lognormal distribution can be used to accurately capture the distribution of *SI* for a given earthquake scenario both over the 'body' and 'tails' of the empirical distribution. The computation of *SI* based on *Sa* prediction equations can be adequately performed using a discretization of the vibration period of less than 0.2 seconds. The proposed approach was verified via comparison with direct prediction equations for *SI*. It was also illustrated that because *Sa* terms at various periods are not perfectly correlated, *SI* is a highly *predictable* IM as compared to other common IMs such as *Sa* and *PGV*.

DATA AND RESOURCES

All data used in this paper came from published sources listed in the references.

ACKNOWLEDGEMENTS

The first author would like to acknowledge funding from the New Zealand Tertiary

Education Commission. Fruitful discussions of the first author with Dr Laurentiu Danciu and Dr Jack Baker during the initial development of this work, and Mr. Nirmal Jayaram near its completion are greatly appreciated.

REFERENCES:

Abrahamson, N. A. and Silva, W. J. (1997). "Empirical response spectral attenuation relations for shallow crustal earthquakes." *Seismological Research Letters* **68**, 94–126.

Abrahamson, N. A. and Silva, W. J. (2008). "Summary of the Abrahamson & Silva NGA ground motion relations." *Earthquake Spectra* **24**, 67-97.

Ang, A. H. S. and Tang, W. H. (1975). *Probability Concepts in Engineering Planning and Design* John Wiley & Sons, Inc.

Baker, J. W. and Cornell, C. A. (2006). "Correlation of Response Spectral Values for Multi-component Ground motions." *Bulletin of the Seismological Society of America* **96**, 215-227.

Baker, J. W. and Jayaram, N. (2008). "Correlation of spectral acceleration values from NGA ground motion models." *Earthquake Spectra* **24**, 299-317.

Boore, D. M. and Atkinson, G. M. (2008). "Ground-motion prediction equations for the average horizontal component of PGA, PGV, and 5%-damped PSA at spectral periods between 0.01s and 10.0s." *Earthquake Spectra* **24**, 99-138.

Bradley, B. A., Cubrinovski, M., Dhakal, R. P. and MacRae, G. A. (2008a). "Evaluation of seismic response of piles within the PBEE framework: liquefiable soils." *Soil Dynamics and Earthquake Engineering (submitted)*.

Bradley, B. A., Cubrinovski, M., Dhakal, R. P. and MacRae, G. A. (2008b). "Evaluation of seismic response of piles within the PBEE framework: non-liquefiable soils." *Soil Dynamics and Earthquake Engineering (submitted)*.

Campbell, K. W. and Bozorgnia, Y. (1994) "Near-source attenuation of peak horizontal acceleration from worldwide accelerograms recorded from 1957 to 1993." *Fifth U.S. National Conference on Earthquake Engineering*, Berkley, California, 283-292.

Campbell, K. W. and Bozorgnia, Y. (2008). "Campbell-Bozorgnia NGA horizontal ground motion model for PGA, PGV, PGD and 5% damped linear elastic response spectra." *Earthquake Spectra* **24**, 139-171.

Danciu, L. and Tselentis, G. A. (2007). "Engineering Ground motion Attenuation Relationships for Greece." *Bulletin of the Seismological Society of America* **97**, 162-183.

Housner, G. W. (1952) "Spectrum intensities of strong-motion earthquakes." *Symposium on earthquakes and blast effects on structures*, Los Angeles, CA.

Housner, G. W. (1963). "The behaviour of Inverted Pendulum Structure During

Earthquake." *Bulletin of the Seismological Society of America* **53**, 403-417.

Inoue, T. and Cornell, C. A. (1990). "Seismic hazard analysis of multi-degree-of-freedom structures."Reliability of Marine Structures, RMS-8, Stanford, CA, 70pp.

Jayaram, N. and Baker, J. W. (2008). "Statistical tests of the joint distribution of spectral acceleration values." *Bulletin of the Seismological Society of America (in press)*.

Johnson, N. L. and Kotz, S. (1972). *Distributions in Statistics: Continuous Multivariate Distributions*, John Wiley & Sons, Inc.

Kramer, S. L. and Mitchell, R. A. (2006). "Ground motion intensity measures for liquefaction hazard evaluation." *Earthquake Spectra* **22**, 413-438.

Shome, N. and Cornell, C. A. (1999). "Probabilistic seismic demand analysis of nonlinear structures." *Report No. RMS-35, RMS Program*, Stanford University, Stanford, CA, 357 pp.pp.

AUTHORS AFFILIATIONS AND ADDRESSES

Brendon A Bradley, PhD Candidate, Department of Civil Engineering, University of Canterbury, Private Bag 4800 Christchurch, New Zealand. Ph. +64 3 364 2987 ext 7333. bab54@student.canterbury.ac.nz . SSA Member

Misko Cubrinovski, Associate Professor, Department of Civil Engineering, University of Canterbury, Private Bag 4800 Christchurch, New Zealand. Ph. +64 3 364 2251. misko.cubrinovski@canterbury.ac.nz

Gregory A MacRae, Associate Professor, Department of Civil Engineering, University of Canterbury, Private Bag 4800 Christchurch, New Zealand. Ph. +64 3 364 2247. gregory.macrae@canterbury.ac.nz

Rajesh P Dhakal, Senior Lecturer, Department of Civil Engineering, University of Canterbury, Private Bag 4800 Christchurch, New Zealand. Ph. +64 3 364 2987 ext 7673. rajesh.dhakal@canterbury.ac.nz

FIGURE CAPTIONS

Figure 1: Distribution of *SI* obtained by simulation compared with normal and lognormal distributions.

Figure 2: Errors in the SI distribution simulation: (a) relative error in the mean and standard deviation; and (b) the Kolmogorov-Smirnov test statistic

Figure 3: Investigation of the tail of the *SI* distribution: (a) comparison between empirical and lognormal distributions for the simulation shown in Figure 1; and (b) the Anderson-Darling test statistic.

Figure 4: Effect of period discretization size on convergence of: (a) median (Equation (11)); and (b) lognormal standard deviation (dispersion) (Equation (12)).

Figure 5: Comparison of *SI* obtained directly from an *SI* prediction equation and that obtained by the proposed method via spectral acceleration prediction equations, both from Danciu and Tselentis (2007).

Figure 6: Comparison of the magnitude of the lognormal standard deviation (dispersion) for spectral accelerations at various periods, *Sa*, peak ground velocity, *PGV*, and spectrum intensity, *SI*.

Figure 7: Variation in lognormal standard deviation (dispersion) as a function of: (a) magnitude; and (b) source-to-site distance.

FIGURES

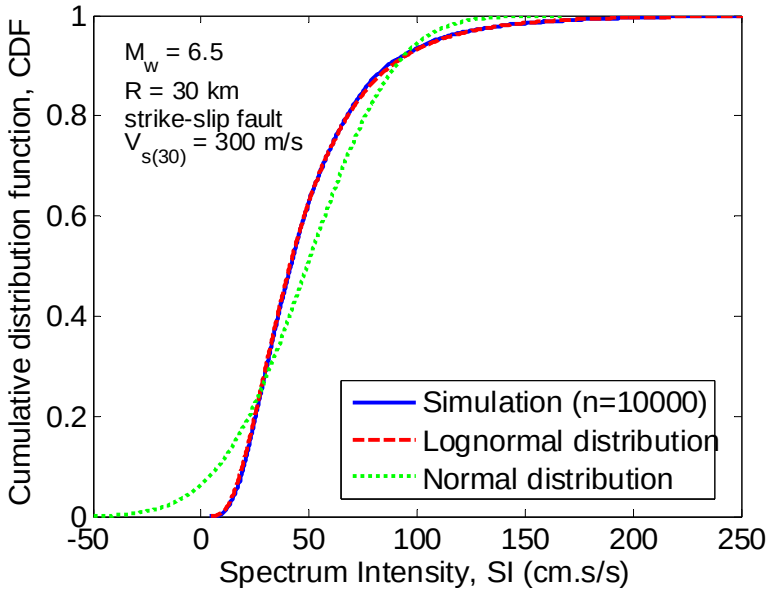

Figure 1: Distribution of *SI* obtained by simulation compared with normal and lognormal distributions.

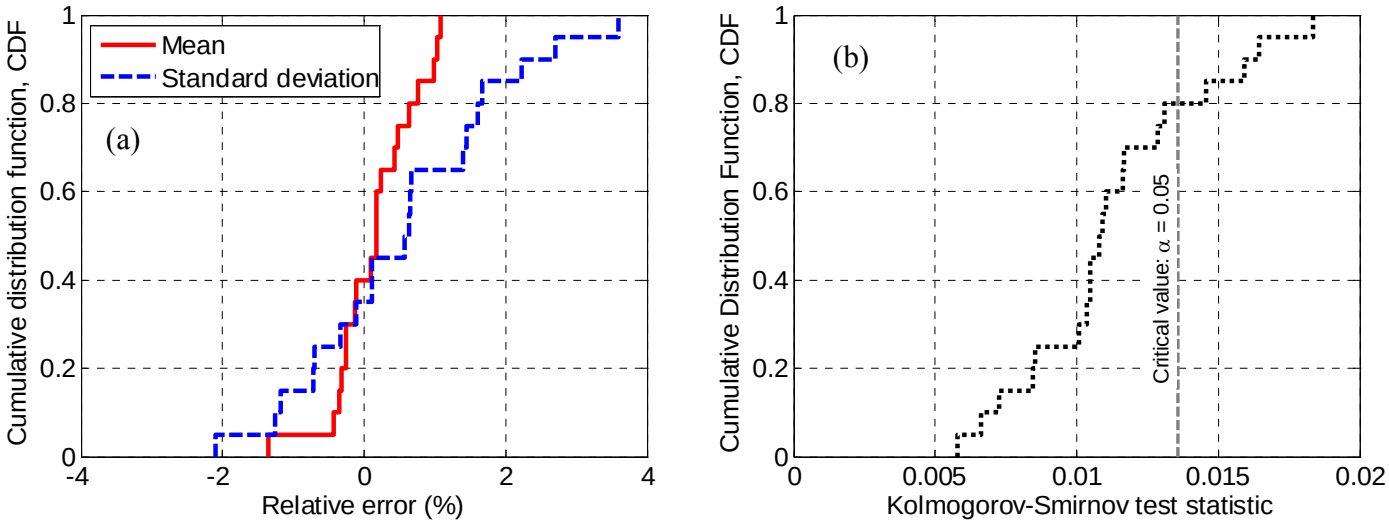

Figure 2: Errors in the SI distribution simulation: (a) relative error in the mean and standard deviation; and (b) the Kolmogorov-Smirnov test statistic

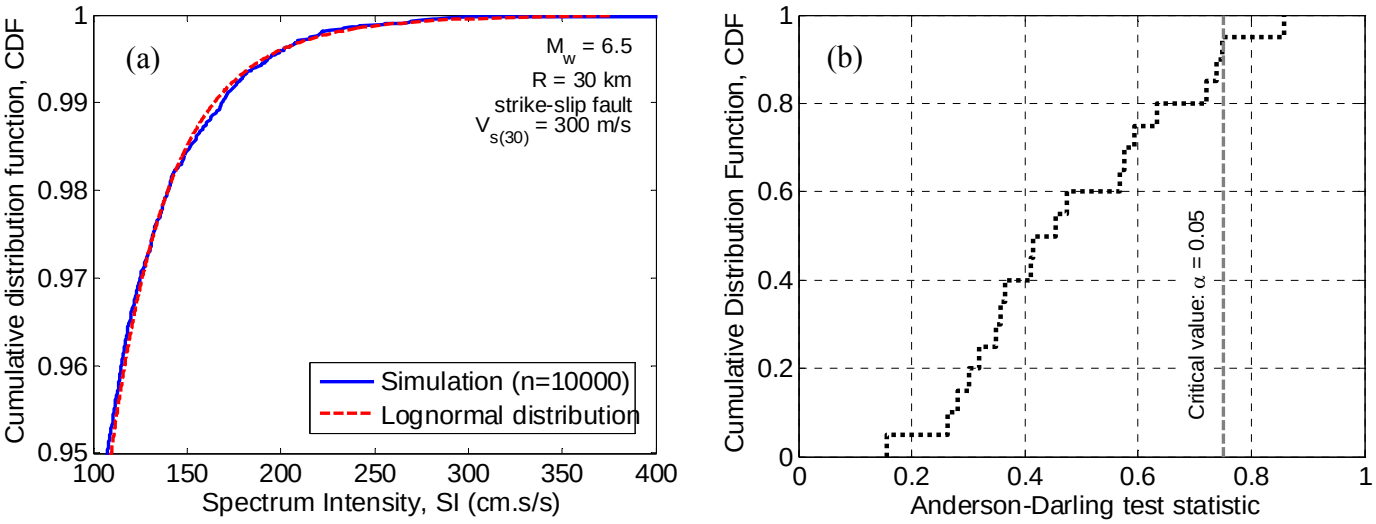

Figure 3: Investigation of the tail of the *SI* distribution: (a) comparison between empirical and lognormal distributions for the simulation shown in Figure 1; and (b) the Anderson-Darling test statistic.

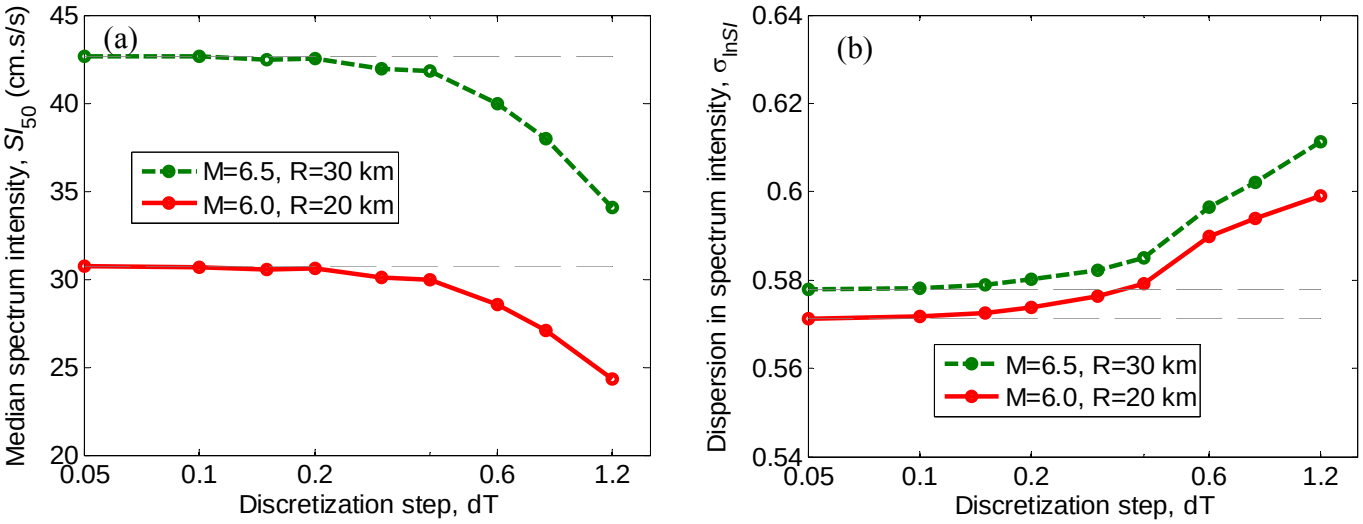

Figure 4: Effect of period discretization size on convergence of: (a) median (Equation (11)); and (b) lognormal standard deviation (dispersion) (Equation (12)).

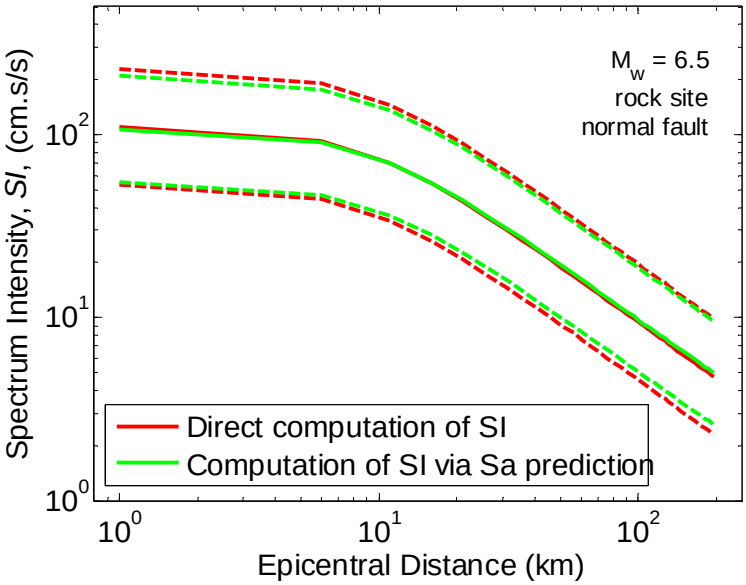

Figure 5: Comparison of *SI* obtained directly from an *SI* prediction equation and that obtained by the proposed method via spectral acceleration prediction equations, both from Danciu and Tselentis (2007).

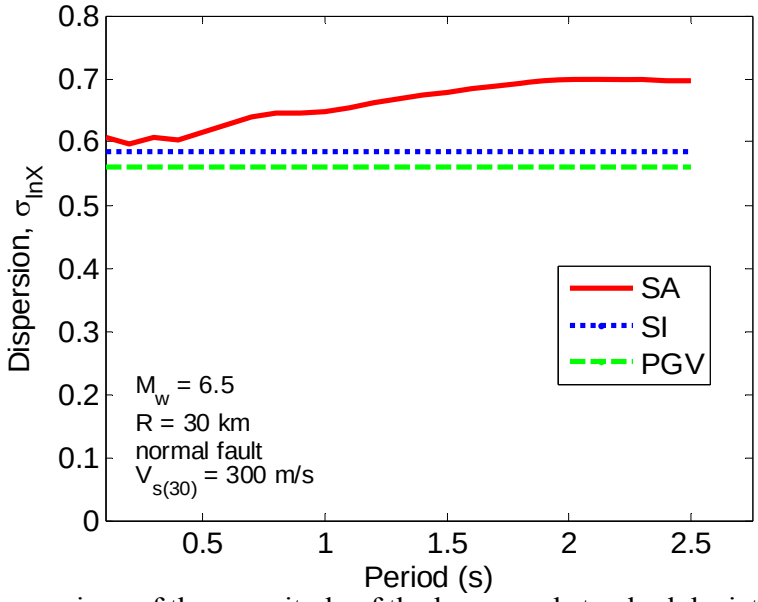

Figure 6: Comparison of the magnitude of the lognormal standard deviation (dispersion) for spectral accelerations at various periods, *Sa*, peak ground velocity, *PGV*, and spectrum intensity, *SI*.

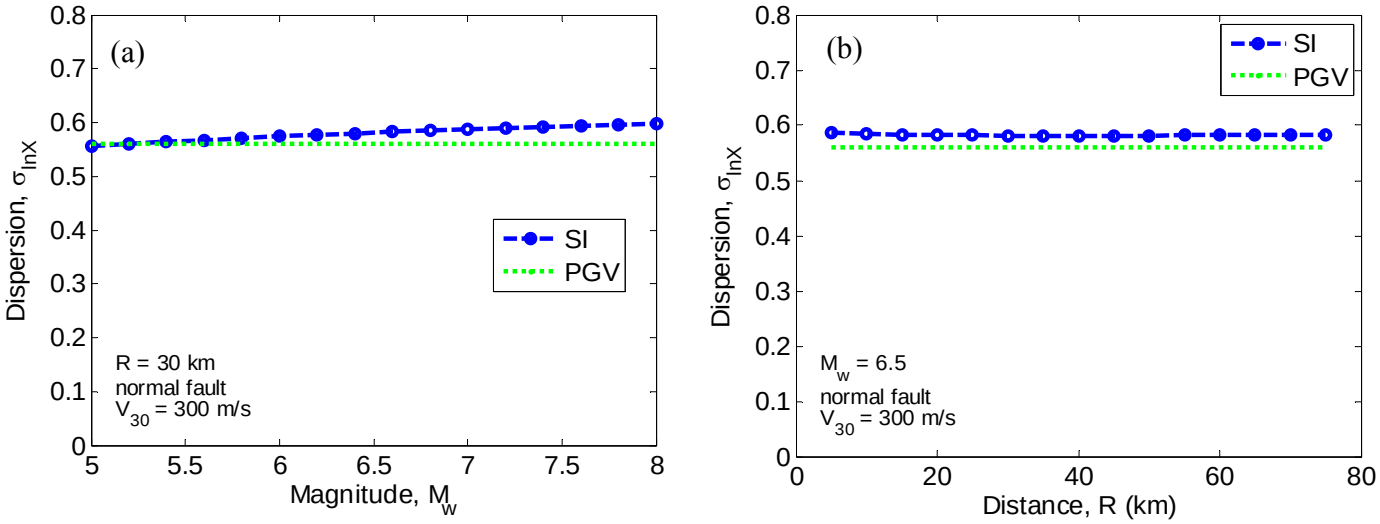

Figure 7: Variation in lognormal standard deviation (dispersion) as a function of: (a) magnitude; and (b) source-to-site distance.

APPENDIX: COMPUTATION OF *PSV* CORRELATION

Given:

$$PSV_i = \frac{1}{\omega_i} Sa_i$$

where $Sa_i = Sa(T = T_i, 5\%)$ is the (pseudo) spectral acceleration; $PSV_i = PSV(T = T_i, 5\%)$ is the pseudo-spectral velocity, and the general expressions:

$$Cov[aX, bY] = abCov[X, Y] = ab\rho_{X,Y}\sigma_X\sigma_Y$$

$$Var[aX] = a^2 Var[X] = a^2\sigma_X^2$$

Then it follows that:

$$\begin{aligned}\rho_{PSV_i,PSV_j} &= \frac{Cov\left[\frac{1}{\omega_i}Sa_i, \frac{1}{\omega_j}Sa_j\right]}{\sqrt{Var\left[\frac{1}{\omega_i}Sa_i\right]Var\left[\frac{1}{\omega_j}Sa_j\right]}} \\ &= \frac{\frac{1}{\omega_i}\frac{1}{\omega_j}\rho_{Sa_i,Sa_j}\sigma_{Sa_i}\sigma_{Sa_j}}{\frac{1}{\omega_i}\sigma_{Sa_i}\frac{1}{\omega_j}\sigma_{Sa_j}} \\ &= \rho_{Sa_i,Sa_j}\end{aligned} \tag{A1}$$

Secondly, the following expressions provide relationships between the moments of the normal and lognormal univariate distributions (Ang and Tang, 1975) (where the substitutions $Y = lnSa$ and $X = Sa$ have been made for brevity):

$$\mu_X = \exp\left(\mu_Y + \frac{1}{2}\sigma_Y^2\right) \tag{A2}$$

$$\sigma_X^2 = \exp\left(2\mu_Y + \sigma_Y^2\right)\left(\exp\left(\sigma_Y^2\right) - 1\right) \tag{A3}$$

Equations (A2) and (A3) can be easily generalised for multivariate distributions to

(Johnson and Kotz, 1972):

$$\mu_{X_i} = \exp\left(\mu_{Y_i} + \frac{1}{2}\sigma_{Y_i}^2 \right) \tag{A4}$$

$$\sigma_{X_i}^2 = \exp\left(2\mu_{Y_i} + \sigma_{Y_i}^2\right)\left(\exp\left(\sigma_{Y_i}^2\right) - 1\right) \tag{A5}$$

$$\sigma_{X_i,X_j} = \exp\left(\mu_{Y_i} + \mu_{Y_j} + \frac{1}{2}\left(\sigma_{Y_i}^2 + \sigma_{Y_j}^2\right)\right)\left(\exp\left(\rho_{Y_i,Y_j}\sigma_{Y_i}\sigma_{Y_j}\right) - 1\right) \tag{A6}$$

Making use of Equation (A4), and that $\sigma_{X_i,X_j} = \rho_{X_i,X_j}\sigma_{X_i}\sigma_{X_j}$, Equation (A6) can be rewritten as:

$$\rho_{X_i,X_j} = \frac{\mu_{X_i}}{\sigma_{X_i}}\frac{\mu_{X_j}}{\sigma_{X_j}}\left(\exp\left(\rho_{Y_i,Y_j}\sigma_{Y_i}\sigma_{Y_j}\right) - 1\right) \tag{A7}$$

The first terms in Equation (A7) are the reciprocal of the coefficient of variation of X_i and X_j, respectively, and can be expressed as a function of Y_i and Y_j using Equations (A4) and (A5):

$$\frac{\sigma_{Xi}}{\mu_{X_i}} = \frac{\sqrt{\exp\left(2\mu_{Y_i} + \sigma_{Y_i}^2\right)\left(\exp\left(\sigma_{Y_i}^2\right) - 1\right)}}{\exp\left(\mu_{Y_i} + \frac{1}{2}\sigma_{Y_i}^2 \right)} = \sqrt{\exp\left(\sigma_{Y_i}^2\right) - 1} \tag{A8}$$

Substituting Equation (A8) into Equation (A7) gives:

$$\rho_{X_i,X_j} = \frac{\exp\left(\rho_{Y_i,Y_j}\sigma_{Y_i}\sigma_{Y_j}\right) - 1}{\sqrt{\exp\left(\sigma_{Y_i}^2\right) - 1}\sqrt{\exp\left(\sigma_{Y_j}^2\right) - 1}} \tag{A9}$$

Further, making the first order Taylor Series approximation $\exp(z) \approx 1 + z + O\left(z^2\right)$ Equation (A9) becomes:

$$\rho_{X_i,X_j} \approx \rho_{Y_i,Y_j} \tag{A10}$$

Thus by substituting $Y = lnSa$ and $X = Sa$, Equation (A11) is obtained, as presented in Equation (10) in the manuscript.

$$\rho_{PSV_i,PSV_j} = \rho_{Sa_i,Sa_j} = \frac{\exp\left(\rho_{\ln Sa_i,\ln Sa_j}\sigma_{\ln Sa_i}\sigma_{\ln Sa_j}\right)-1}{\sqrt{\exp\left(\sigma^2_{\ln Sa_i}\right)-1}\sqrt{\exp\left(\sigma^2_{\ln Sa_j}\right)-1}} \approx \rho_{\ln Sa_i,\ln Sa_j} \quad \text{(A11)}$$